5062 *Macromolecules* **2009**, *42*, 5062–5072
DOI: 10.1021/ma900774e

Macromolecules
ARTICLE

Influence of Ionic Liquid Structure on the Propagation Kinetics of Methyl Methacrylate

Aleksandra Jeličić,[†] Sabine Beuermann,*[,†] and Nuria García[‡]

[†]*Institute of Chemistry, University of Potsdam, Karl-Liebknecht Str. 24-25, 14476 Golm, Potsdam, Germany, and* [‡]*Instituto de Ciencia y Tecnología de Polímeros (CSIC), Juan de la Cierva 3, 28006 Madrid, Spain*

Received April 9, 2009; Revised Manuscript Received June 2, 2009

ABSTRACT: Propagation rate coefficients, k_p, of methyl methacrylate, MMA, homopolymerizations in ionic liquids (ILs) with widely varying structures and physical properties were determined applying the so-called PLP-SEC technique, which combines pulse-laser initiation of the polymerization (PLP) with molecular weight analysis via size-exclusion chromatography (SEC). For all ILs a strong enhancement of k_p and a decrease in the activation energy of k_p compared to the bulk system were observed. Depending on the IL structure, the increase in k_p is between a factor of 2 and 4. Both the cation and the anion are responsible for the enhancement of k_p. The smaller the ions of the ILs, the stronger the enhancement of k_p. Investigations into the solvent properties of ILs using a solvatochromic dye and infrared spectroscopy suggest that electron pair acceptor−electron pair donator interactions and nonspecific (Coulomb) interactions contribute strongly to the solvent influence, whereas contributions from H bonding are negligible. The knowledge of normalized polarity values of the ILs allows for a rough estimate of the IL-induced variation of k_p.

Introduction

The solvent influence on polymerization kinetics was discussed in a large number of publications, e.g., in refs 1−12. It was shown that the solvent may increase or lower k_p and that the extent of change may vary from a few percent to more than 1 order of magnitude. With the development of the PLP-SEC method, which combines pulsed laser initiated polymerization (PLP) with subsequent polymer analysis via size-exclusion chromatography (SEC), by Olaj and co-workers[13] reliable propagation rate coefficients were accessible. The PLP-SEC technique was recommended as the method of choice for the determination of k_p by the IUPAC Working Party on "Modeling of Polymerization Kinetics and Processes".[14] k_p is derived according to eq 1:

$$L_i = ik_p c_M t_0 \qquad i = 1, 2, 3, ... \tag{1}$$

where c_M is the monomer concentration, t_0 the time between two successive laser pulses, and L_1 is the number of propagation steps between two pulses. L_1 is calculated according to $L_1 = M_1/M_{MMA}$, where M_{MMA} is the molar mass of the monomer and M_1 may be identified by the first inflection point of the molecular weight distribution (MWD).[13,15] To derive reliable k_p values, the existence of a second or even a third inflection point at degrees of polymerization around $L_2 = 2L_1$ and $L_3 = 3L_1$ is required. These higher order inflection points serve as a consistency criterion for k_p determination via PLP-SEC.[16]

Since the introduction of PLP-SEC, in particular propagation rate coefficients of methyl methacrylate, MMA, were studied in a wide variety of solvents.[3,4,9,17−19] Up to now, the strongest influence of conventional organic solvents on k_p was reported for dimethyl sulfoxide[4] and benzyl alcohol,[4,18] where k_p was by a factor of 2 higher than the associated bulk value. Recently, the influence of ionic liquids, ILs, on polymerization kinetics was investigated.[20−22] In all cases a strong enhancement of MMA k_p was found, e.g., for polymerizations in 1-ethyl-3-methylimidazolium ethylsulfate, [EMIM][$EtSO_4$]; k_p is 4 times as high as the associated bulk value.[22] The diffusion-controlled MMA termination rate coefficients decreased by up to 1 order of magnitude as the concentration of 1-butyl-3-methylimidazolium hexafluorophosphate, [BMIM][PF_6], was raised to 60 vol %.[21] A recent study on the IL influence on polymerizations of poly(ethylene glycol) methacrylate monomers reports an enhancement of the propagation rate and a decrease in termination rate.[23] In addition, several studies showed that polymer molecular weights are significantly increased when polymerizations are carried out in ILs.[24,25]

Woecht et al.[22] reported that the IL influence on k_p strongly depends on the type of monomer and IL used. IL polarity was suggested to be the most probable origin of the k_p enhancement.[21,22] To be able to fully exploit the IL influence on polymerization processes and to optimize and model polymerization reactions, a deeper understanding of the IL-induced k_p enhancement is required.

Apart from their influence on polymerization kinetics, ILs exhibit many other interesting characteristics, e.g., high thermal stability, liquid salts consisting of mobile ions, and a broad temperature range where the substances are liquid.[26−30] The solvent properties may be tuned by changing the nature of cation and/or anion. Moreover, frequently ILs are considered as green solvents due to their negligible vapor pressure.[31] As reviewed by Kubisa, various types of polymerization may be carried out in ILs.[32] Advantages of ILs as reaction media are seen in easy removal of catalyst[33] and the suppression of side reactions. Particularly interesting are applications toward functional polymers, e.g., polymer gels based on ILs, ILs as scaffolds for porous materials, or electrochemical polymerizations in ILs.[34]

This publication reports a systematic study on the influence of ILs with widely varying cation and anion structures on the propagation kinetics of MMA. The following ILs were chosen: 1-hexyl-3-methylimidazolium chloride, [HMIM]-Cl, 1-ethyl-3-methylpyridinium nonafluorobutylsulfonate,

*To whom correspondence should be addressed.

 Published on Web 06/26/2009

Scheme 1. Ionic Liquids Used as Solvent for MMA Polymerizations

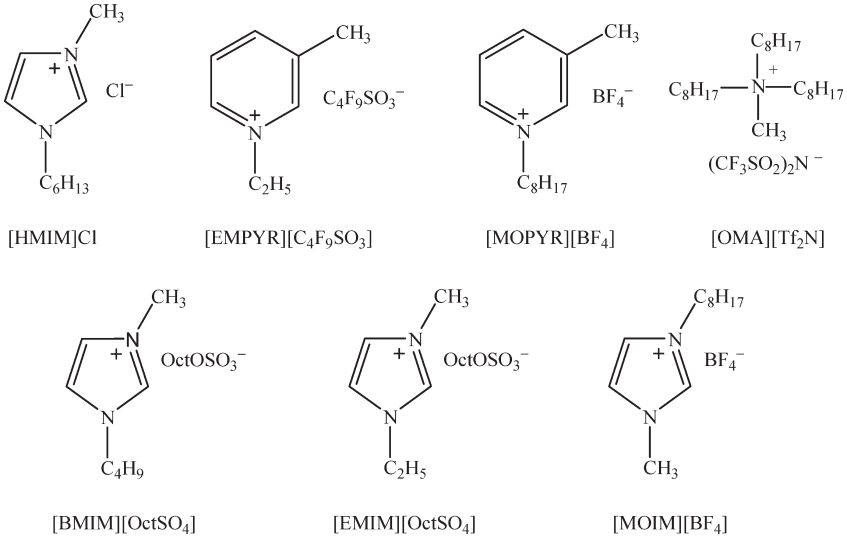

[EMPYR][$C_4F_9SO_3$], 3-methyl-1-octylpyridinium tetrafluoroborate, [MOPYR][BF_4], trioctylmethylammonium bis(trifluoromethylsulfonyl) imide, [OMA][Tf_2N], 1-butyl-3-methylimidazolium *n*-octylsulfate, [BMIM][$OctSO_4$], 1-ethyl-3-methylimidazolium *n*-octylsulfate, [EMIM][$OctSO_4$], and 1-methyl-3-octylimidazolium tetrafluoroborate, [MOIM][BF_4]. The structures of these ILs are depicted in Scheme 1.

To explain the origin of the IL-induced k_p enhancement, intermolecular interactions in monomer/solvent mixtures are investigated by Fourier-transform infrared spectroscopy (FT-IR). UV−vis spectra of a solvatochromic dye dissolved in ILs and mixtures of MMA and IL are recorded to measure the polarity. Unlike consideration of a single physical parameters such as dielectric constant, dipole moment, or refractive index, the employment of solvatochromic dyes was recommended for observation of the solvation capabilities of ILs.[35,36] The method allows for taking into account specific and nonspecific intermolecular forces between solvent and solute.

Experimental Section

Materials. Methyl methacrylate (MMA, Aldrich, 99%) for pulsed laser initiated polymerizations was distilled under high vacuum before use to remove the inhibitor. The photoinitiator, 2-methyl-4′-(methylthio)-2-morpholinopropiophenone (MMMP, Aldrich, 98%), 2,6-diphenyl-4-(2,4,6-triphenyl-1-pyridinio)phenolate (Reichardt's dye, Fluka, techn ≥90%), and the ionic liquids 1-hexyl-3-methylimidazolium chloride ([HMIM]Cl, Fluka, ≥97%, or Solvent Innovation, 98%), 1-butyl-3-methylimidazolium *n*-octylsulfate ([BMIM][$OctSO_4$], Fluka, ≥95%), trioctylmethylammonium bis(trifluoromethylsulfonyl)imide ([OMA][Tf_2N], Fluka, ≥99%, Solvent Innovation, 98%, or IoLiTec, 99%), 3-methyl-1-octylpyridinium tetrafluoroborate ([MOPYR][BF_4], Solvent Innovation, 99%), 1-ethyl-3-methylpyridinium nonafluorobutylsulfonate ([EMPYR][$C_4F_9SO_3$], Solvent Innovation, 99%), 1-ethyl-3-methylimidazolium *n*-octylsulfate ([EMIM][$OctSO_4$], Solvent Innovation, 98%), and 1-methyl-3-octylimidazolium tetrafluoroborate ([MOIM][BF_4], Solvent Innovation, 99%) were used as received. The kinetic parameters derived are independent of the IL supplier. Methanol (VWR, 99%) containing trace amounts of hydroquinone (Fluka, 98%) was used to precipitate the polymer and tetrahydrofuran (Scharlau, GPC grade) as eluent for SEC. The initiator 2,2′-azobis(isobutyronitrile) (AIBN, Fluka, 98%) was purified by recrystallization from methanol prior to use.

Pulsed Laser Initiated Polymerization. Pulsed laser initiated polymerizations were carried out at temperatures ranging from 10 to 60 °C using a thermostated cuvette (Hellma 165 QS, 10 mm path length). Temperature was controlled via a thermostat with a recirculating mixture of water and ethylene glycol. The temperature was monitored during laser irradiation using a digital thermometer (Testo 735-2) equipped with a 1 mm diameter external probe placed inside the cell and located at the center of the laser beam pathway. The response time and the precision of the instrument are 1 s and ±0.1 °C, respectively. (Note: irradiation of the thermometer at the same conditions as the PLP experiments in an inert medium did not result in a variation in temperature.) As a representative reaction temperature, the arithmetic mean temperature, T, of the sequentially registered temperatures was considered. The difference between the initial and the final temperature during PLP ranges from 0.4 to 2.5 °C depending on IL type and concentration as well as on the initial temperature. The importance of monitoring the temperature during PLP was pointed out by García et al.[37] MMA k_p data from ref 37 were taken for comparison with the k_p values determined in this study as the majority of PLP experiments were conducted under the same experimental conditions as in ref 37.

Monomer/IL solutions with MMMP concentrations ranging from 0.3 to 5 mmol L^{-1} were prepared. Polymerization was induced using a Quanta-Ray Nd:YAG laser (Spectra-Physics) operating at 355 nm with a pulse repetition rate, ν_{rep}, of 5 Hz and a pulse energy, E_p, of ∼17 mJ. A Stanford DG 535 pulse delay generator was used to adjust the pulse repetition rate. The pulsing time was chosen such that the conversion of monomer does not exceed 10%. The polymer was precipitated in methanol containing traces of hydroquinone to prevent further polymerization, washed twice with methanol to remove the ionic liquid, and dried in vacuum prior to SEC analysis.

A small number of polymerizations were carried out at room temperature without monitoring temperature during irradiation (protocol B). The polymerization was initiated using a Q-switched Nd:YAG laser (B.M. Industries, 5000 series) operating at 355 nm with ν_{rep} of 5 or 10 Hz and pulse energies of 6 or 36 mJ. The IL was removed from polymer either by washing the sample twice with methanol or using cellulose dialysis tubing (Spectra/Por 6, molecular weight (MW) cutoff 2000). The work-up did not influence the k_p values. Thus, the majority of samples were washed with methanol. Polymers purified by dialysis are marked with an asterisk in Tables S1−S6 in the Supporting Information.

Size-Exclusion Chromatography. Molecular weight distributions, MWDs, were obtained by size-exclusion chromatography

Table 1. Density Parameters ρ_0 and b (Eq 2) of Neat MMA and MMA/IL Mixtures with the Monomer Concentration, c_M, at 25 °C

solvent	c_M (25 °C) (mol L^{-1})	ρ_0 (g mL^{-1})	$b \times 10^4$ (g mL^{-1} °C^{-1})
bulk		0.966	11.70
[OMA][Tf_2N]	2.1	1.090	8.268
[OMA][Tf_2N]	3.2	1.073	8.730
[OMA][Tf_2N]	5.0	1.043	9.462
[OMA][Tf_2N]	7.0	0.998	10.50
[MOPYR][BF_4]	2.1	1.086	9.084
[MOPYR][BF_4]	3.3	1.068	7.989
[MOPYR][BF_4]	5.2	1.040	8.940
[MOPYR][BF_4]	7.1	1.010	10.10
[EMPYR][$C_4F_9SO_3$]	2.1	1.412	10.70
[EMPYR][$C_4F_9SO_3$]	3.2	1.324	11.10
[EMPYR][$C_4F_9SO_3$]	5.2	1.229	11.20
[EMPYR][$C_4F_9SO_3$]	7.1	1.113	11.60
[HMIM]Cl	2.1	1.040	7.170
[BMIM][$OctSO_4$]	2.1	1.059	7.387

using a Waters 1515 HPLC pump, a Waters 2414 refractive index detector, and a set of three Waters columns with nominal pore sizes of 10^2, 10^4, and 10^6 Å. Tetrahydrofuran at 35 °C and a flow rate of 1 mL min^{-1} was used as eluent. The SEC setup was calibrated against polystyrene, PS, standards of narrow polydispersity (MW between 580 and 5×10^6 g mol^{-1}, Polymer Standards Services (PSS)). Absolute molecular weights of the polymer samples were calculated via the principle of universal calibration using the Mark−Houwink parameters $K = 11.4 \times 10^{-5}$ dL g^{-1} and $a = 0.716$ for PS[38] as well as $K = 9.44 \times 10^{-5}$ dL g^{-1} and $a = 0.719$ for PMMA.[39]

Polymers prepared according to protocol B were analyzed using an Agilent 1200 isocratic pump, an Agilent 1200 refractive index detector, and two GRAM columns (10 μm, 8 × 300 mm, pore sizes 100 and 1000) from PSS. *N*,*N*-dimethylacetamide (Acros, 99%) containing 0.1% LiBr at 45 °C at a flow rate of 1 mL min^{-1} was used as eluent. The SEC setup was calibrated against PMMA standards of narrow polydispersity (MW between 500 and 1×10^6 g mol^{-1}, PSS). Generally excellent agreement of data from both SEC setups was observed. The deviations in k_p were at most 8%.

Density Measurements. Densities of monomer/IL mixtures required for calculation of the monomer concentration were determined in a temperature range from 10 to 70 °C using an Anton Paar SVM 3000 instrument for various monomer concentrations used in PLP. The experimental density data were fit by a linear relation according to eq 2:

$$\rho/(\text{g mL}^{-1}) = \rho_0 - bT/°\text{C} \quad (2)$$

Monomer concentrations of the MMA/IL mixtures at 25 °C and the corresponding density parameters ρ_0 and b from eq 2 are listed in Table 1.

As the density measurements of MMA/IL mixtures showed negligible excess volumes for the systems in Table 1, in case of MMA/IL mixtures with [EMIM][$OctSO_4$] and [MOIM][BF_4] ideal mixing was assumed and densities of the pure compounds were used to calculate c_M.

FT-IR/NIR Spectroscopy. To monitor monomer conversion, NIR spectra were recorded on a Bruker Vertex 70 spectrometer equipped with a tungsten lamp, a CaF_2 beam splitter, and a liquid nitrogen cooled InSb detector with a resolution of 2 cm^{-1}, a zero-filling factor of 2, and coaddition of 100 scans. The spectrometer is operated by OPUS 6.0 software.

To evaluate solvent−solute interactions, the spectrometer's globar source and a DTGS detector were used to record IR spectra between 1200 and 4000 cm^{-1} with a resolution of 2 cm^{-1}, a zero-filling factor of 2, and coaddition of 32 scans per spectrum. Film spectra of pure MMA and MMA/IL mixtures were measured between two CaF_2 windows.

UV−vis Measurements. Absorption spectra of Reichardt's dye dissolved in MMA, ILs, and in MMA/IL mixtures were recorded on a Perkin-Elmer Lambda 750 absorption spectrometer. The spectra were recorded in Hellma QS quartz cuvettes with 1 mm path length in the wavelength range from 300 to 1000 nm at room temperature. The concentration of the solvatochromic dye was chosen such that the absorbance of the longest wavelength intramolecular charge−transfer $\pi-\pi^*$ absorption band is in the range from 0.5 to 2. Normalized polarity values, E_T^N, which range from 0.0 for tetramethylsilane to 1.0 for water, were calculated using eq 3:[35]

$$E_T^N = \frac{E_T(30) - 30.7}{32.4} \quad (3)$$

where $E_T(30)$ is the molar transition energy of the standard betaine dye no. 30 (Reichardt's dye) and is given by eq 4:[35]

$$E_T(30)\ (\text{kcal mol}^{-1}) = \frac{28591}{\lambda_{max}\ (\text{nm})} \quad (4)$$

λ_{max} is the wavelength of the maximum of the longest wavelength intramolecular charge−transfer $\pi-\pi^*$ absorption band of Reichardt's dye.

As Reichardt's dye is sensitive to the presence of acid, a few microliters of triethylamine was added to [EMIM][$EtSO_4$], [EMIM][$HexSO_4$], [HMIM]Cl, and [EMPYR][$C_4F_9SO_3$] to scavenge acid that may protonate the phenoxide form.[40] Control experiments showed that even addition of 5 wt % of triethylamine did not shift the absorption maximum.

Chemically Initiated Polymerizations. Inhibitor-free MMA and the solvent (IL or toluene) were purged separately to avoid loss of volatile MMA from the mixture. AIBN was dissolved in MMA under a nitrogen atmosphere. The solution of 1 wt % AIBN in MMA was mixed with the required amount of solvent. The polymerization solution was filled into an optical cell (Specac, liquid cell 20510 series) with CaF_2 windows, a 1 mm Teflon spacer, and a heating jacket (Specac, 20730) fitted with a low-voltage heater powered by a 4000 Series temperature controller. Prior to filling, the cell was flashed with argon. The thermostated cell at 60 °C containing the reaction mixture was inserted into the sample compartment of the FT-IR/NIR spectrometer, and a series of NIR spectra was recorded. The first overtone of the C−H stretching vibration of the C=C double bond at around 6168 cm^{-1} was used to monitor and calculate MMA conversion as a function of polymerization time.[41] To eliminate contributions from absorptions of the solvent, the spectrum for complete MMA conversion was subtracted from each spectrum recorded during the course of polymerization. c_M was calculated by integration over the high wavenumber half-band from the maximum at around 6168 cm^{-1} over a range of 70 cm^{-1} toward higher wavenumbers, against a horizontal baseline at 6300 cm^{-1}.

Results

Monomer Conversion vs Time. Solution polymerizations of MMA were carried out in an optical cell allowing for in-line monitoring of monomer conversion via FT-NIR spectroscopy. Figure 1 gives the conversion−time data for MMA polymerizations in [OMA][Tf_2N] and [MOPYR][BF_4]. For comparison data from a polymerization in toluene are included, too. In all cases c_M was 5 mol L^{-1}, and the initiator concentration, c_{AIBN}, was 1.0 wt % relative to the monomer.

Figure 1 shows that MMA polymerizations in [OMA][Tf_2N] and [MOPYR][BF_4] may be carried out up to complete monomer conversion in the homogeneous phase. In case of heterogeneity the detection of monomer conversion via FT-NIR would have failed. This finding is remarkable,

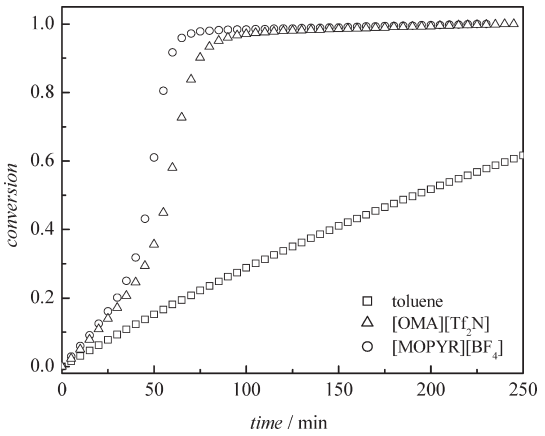

Figure 1. Conversion vs time for MMA polymerizations at 60 °C in toluene, [OMA][Tf_2N], and [MOPYR][BF_4] with c_M = 5 mol L^{-1}, and c_{AIBN} = 1.0 wt % relative to the monomer.

since polymer solubility in ILs is often rather low;[33,42] e.g., butyl methacrylate polymerizations in 29 ILs always resulted in precipitation of the polymer,[25] and PLP-SEC experiments of glycidyl methacrylate were largely restricted by polymer solubility in ILs.[22] It is also obvious that the initial slope of the conversion−time curves for MMA polymerizations in ILs is steeper than for MMA polymerization in toluene, indicating a higher polymerization rate in the presence of ILs. Moreover, at around 20% conversion an increase in slope is observed for reactions in ILs, whereas the data from MMA polymerization in toluene do not show any significant change in the slope and consequently in rate. Complete conversion was reached in 80 and 110 min for the MMA polymerizations in [MOPYR][BF_4] and [OMA][Tf_2N], respectively, whereas only about 30% MMA conversion is found for polymerization in toluene after 110 min. The higher initial polymerization rate for reactions in [OMA][Tf_2N] and in [MOPYR][BF_4] as well as the occurrence of the gel effect at around 20% conversion may be explained by the influence of the IL-induced higher viscosity on the diffusion-controlled termination rate coefficient. Further, the anticipated enhancement of k_p due to the presence of the ILs will contribute to the higher polymerization rate.

In contrast to polymerizations in [OMA][Tf_2N] and [MOPYR][BF_4], which proceed homogeneously until complete monomer conversion, MMA polymerization in [MOIM][BF_4] may be performed in homogeneous phase only for c_M > 5 mol L^{-1}. In polymerizations of all other mixtures the solution turned heterogeneous at conversions higher than 10%. In contrast to all other systems that showed miscibility of monomer and IL at all concentrations, MMA/[HMIM]Cl systems were homogeneous for c_M < 3 mol L^{-1} only.

Variation of k_p with Monomer Concentration. The variation of k_p with c_M was investigated in detail for the MMA/[OMA][Tf_2N] and the MMA/[MOPYR][BF_4] systems, which allowed for polymerization in homogeneous phase up to complete monomer conversion. In addition, the MMA/[EMPYR][$C_4F_9SO_3$] system was investigated over an extended range of monomer concentrations serving as a representative of the systems that turned heterogeneous at conversions above ~10% conversion. c_M was varied between 2 and 7 mol L^{-1}. Details of each experiment and k_p values derived in this work are listed in Tables S1−S6 in the Supporting Information. The tables give the photoinitiator concentration, c_{MMMP}, the energy per pulse, E_p, the

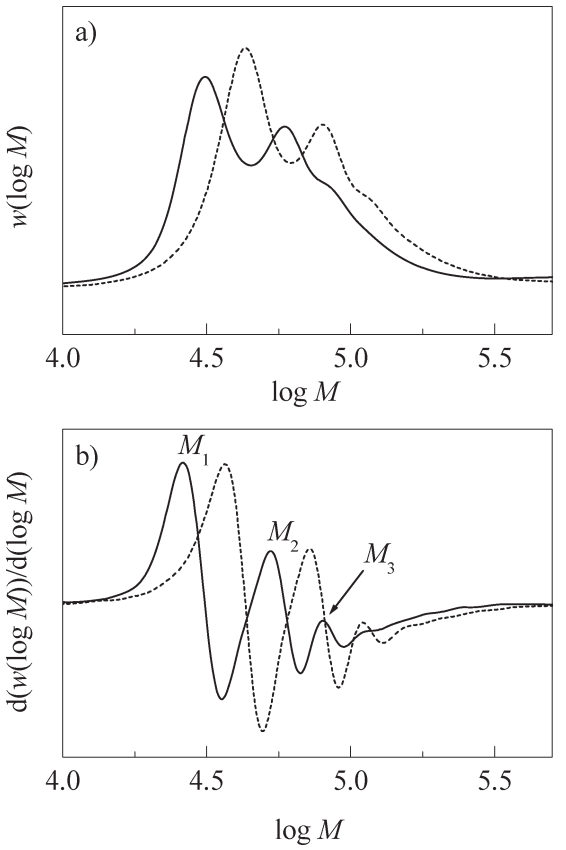

Figure 2. Molecular weight distributions (a) and associated first derivative curves (b) for PMMA obtained from MMA PLP in [OMA][Tf_2N] with c_M = 2.14 mol L^{-1} (full line) and 3.20 mol L^{-1} (dotted line) at 27 °C.

polymerization temperature, T, and the molecular weights at the first and second inflection point, M_1 and M_2, respectively. In all cases the ratio of M_1/M_2 is ~0.5, fulfilling the PLP consistency criteria. In addition, variations in initiator concentration, laser pulse energy, and pulse repetition rate did not affect the kinetic results.

As an example, Figure 2 shows the MWDs (a) and the associated first derivatives of the MWDs (b) of PMMA obtained from PLP with 2.14 and 3.20 mol L^{-1} of MMA in [OMA][Tf_2N]. The MWDs show two clear maxima and a shoulder. The corresponding derivative curves clearly exhibit three maxima indicative of inflection points of the MWDs. The position of inflection points in Figure 2b is indicated by M_1, M_2, and M_3 for the lower c_M.

To allow for comparison of k_p values determined at slightly different temperatures between 23 and 27 °C, Figure 3 presents k_p values for polymerizations in ILs relative to the corresponding bulk values. In addition, data from Harrisson et al.[21] for MMA polymerizations in [BMIM][PF_6] at T~ 25 °C are depicted as a function of c_M. For clarity of presentation, arithmetic mean values at each c_M are given. In all cases a strong enhancement of k_p with increasing IL content is observed.

It is evident that $k_p/k_{p,bulk}$ is the lowest for MMA polymerizations in [OMA][Tf_2N] over the entire range of monomer concentrations. Differences in k_p for MMA polymerizations in [EMPYR][$C_4F_9SO_3$] and [MOPYR][BF_4] may be observed at c_M lower than 4 mol L^{-1}. The highest value for $k_p/k_{p,bulk}$ at c_M = 2 mol L^{-1} is observed for the MMA/[HMIM]Cl system, where k_p is 3.8 times as high as the associated bulk value. [OMA][Tf_2N] has the weakest

effect on k_p as k_p is only by a factor of 2 above MMA bulk k_p. k_p values for polymerizations in [EMPYR][$C_4F_9SO_3$], [MOPYR][BF_4], and [BMIM][$OctSO_4$] are all very similar and in between k_p for systems containing [OMA][Tf_2N] or [HMIM]Cl.

For comparison to the literature data, arithmetic mean values for $k_p/k_{p,bulk}$ at $c_M = 2$ mol L^{-1} determined in this study and $k_p/k_{p,bulk}$ data from ref 22 for MMA polymerizations in [EMIM][$EtSO_4$], [EMIM][$HexSO_4$], [BMIM][BF_4], and [BMIM][PF_6] are listed in Table 2. With the exception of polymerizations in [HMIM]Cl $k_p/k_{p,bulk}$ values from Table 2 show that the ratio is the highest for the ILs composed of both small cation and anion. As either the size of cation or anion increases, $k_p/k_{p,bulk}$ is lowered. The smallest $k_p/k_{p,bulk}$ value was derived for MMA polymerizations in [OMA][Tf_2N], which is significantly more bulky than the other ILs.

Temperature Dependence of k_p. The temperature dependence of k_p was investigated for the lowest monomer concentration of $c_M = 2$ mol L^{-1}. k_p values and full experimental details are given in the Supporting Information in Tables S1−S6. The data for MMA k_p in [OMA][Tf_2N], [MOPYR][BF_4], [HMIM]-Cl, [BMIM][$OctSO_4$], and [EMPYR][$C_4F_9SO_3$] together with the bulk values[36] are plotted in Figure 4 according to the Arrhenius equation (eq 5):

$$\ln k_p = \ln A - E_a/RT \quad (5)$$

with the pre-exponential factor A and the activation energy E_a. The dashed lines represent linear fits of each experimental data set. The variation of k_p with $1/T$ is similar for all MMA/IL systems except for polymerizations in [EMPYR][$C_4F_9SO_3$], for which a slightly lower variation is found.

To account for experimental uncertainties, 95% joint confidence intervals (JCIs) of the Arrhenius parameters A and E_a were calculated using the program Contour.[46] The JCIs derived on the basis of estimated constant relative errors are plotted in Figure 5. For clarity of presentation the data are given in two separate graphs. The number of data points obtained for each system, the temperature interval for k_p determination, A and E_a derived with the Contour program, and k_p values at 25 °C calculated from the given A and E_a values are listed in Table 3. The JCIs for polymerizations in [OMA][Tf_2N], [BMIM][$OctSO_4$], and [HMIM]Cl in Figure 5a do not overlap with the corresponding JCI for bulk systems. Figure 5a indicates that the pre-exponential is only slightly above the bulk value, whereas a clear decrease in E_a due to the presence of the ILs is observed. Similar results are

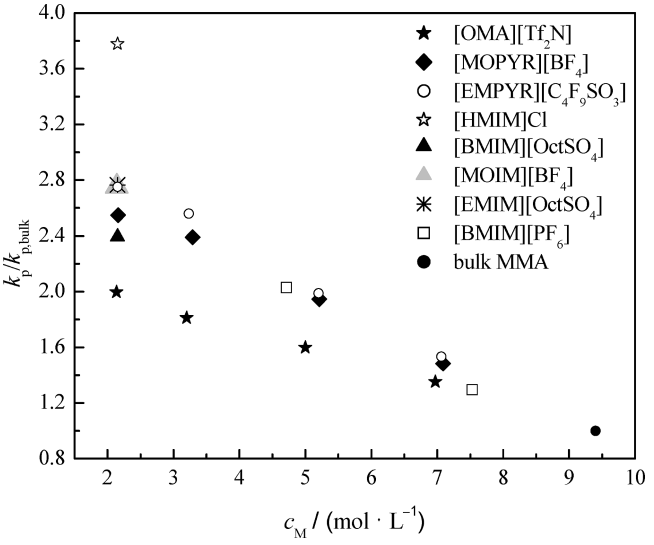

Figure 3. Propagation rate coefficient, k_p, for polymerizations in ILs at 25 ± 2 °C relative to the bulk rate coefficient, $k_{p,bulk}$, vs monomer concentration, c_M, for MMA polymerizations in [OMA][Tf_2N], [MOPYR][BF_4], [EMPYR][$C_4F_9SO_3$], [BMIM][$OCtSO_4$], [HMIM]Cl, [EMIM][$OctSO_4$], [MOIM][BF_4], and [BMIM][PF_6].[21]

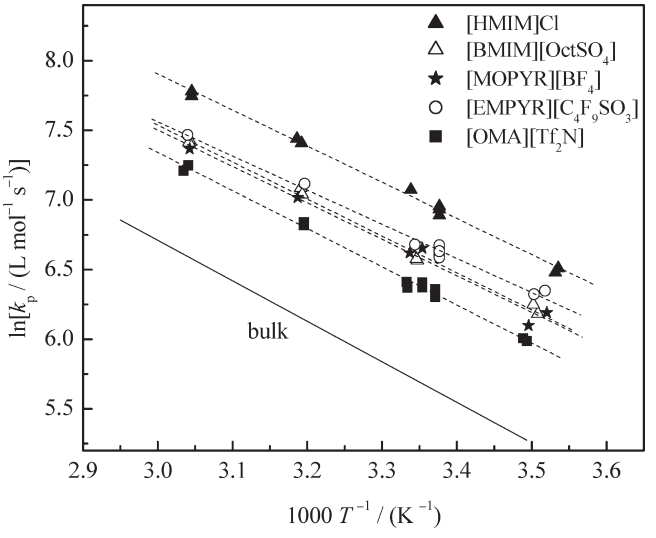

Figure 4. Temperature dependence of k_p for MMA polymerizations in bulk[36] and in [OMA][Tf_2N], [HMIM]Cl, [BMIM][$OctSO_4$], [MOPYR]-[BF_4], or [EMPYR][$C_4F_9SO_3$] with $c_M = 2$ mol L^{-1}.

Table 2. Arithmetic Mean Values of $k_p/k_{p,bulk}$ for MMA Polymerizations in ILs with MMA Concentrations of 2 mol L^{-1}, FTIR Peak Positions of the Carbonyl, ν_{max}(C=O), and the Olefinic Vibration, ν_{max}(C=C), Half-Width of the Carbonyl Peak, $I_{1/2}$, E_T^N Calculated According to Eqs 3 and 4, Anion Volume, V_a, and Cation Volume, V_c

IL	$k_p/k_{p,bulk}$	ν_{max}(C=O)/cm^{-1}	$I_{1/2}$	ν_{max}(C=C)/cm^{-1}	λ_{max}/nm	E_T^N	V_a/Å^3	V_c/Å^3
[EMIM][$EtSO_4$]	3.9[a]	1720	9.7	1636	545	0.67	147[c]	182[c]
[EMIM][$HexSO_4$]	3.1[a]	1722	9.9	1637	549	0.66	259[d]	182[c]
[EMIM][$OctSO_4$]	2.8	1723	9.8	1638	559	0.63	315[d]	182[c]
[BMIM][BF_4]	3.8[a]	1720	10.1	1637	546[b]	0.67[b]	73[c]	238[c]
[BMIM][PF_6]	3.5[a]	1720	10.7	1637	549[b]	0.66[b]	107[c]	238[c]
[BMIM][$OctSO_4$]	2.4	1724	8.9	1638	557	0.64	315[d]	238[c]
[HMIM]Cl	3.8	1721	9.7	1637	574	0.59	47[c]	294[c]
[MOIM][BF_4]	2.8	1722	9.7	1638	554	0.65	73[c]	350[c]
[MOPYR][BF_4]	2.5	1721	9.6	1637	569	0.60	73[c]	370[c]
[EMPYR][$C_4F_9SO_3$]	2.8	1721	10.7	1638				202[d]
[OMA][Tf_2N]	2.0	1721	11.7	1639	621	0.47	230[c]	> 600[d]
MMA	1.0	1726	9.1	1639	748	0.23		

[a] Data from ref 22. Determined at 40 °C. [b] E_T^N range covering the data from refs 35 and 43. [c] Taken from ref 44. [d] Calculated according to ref 45.

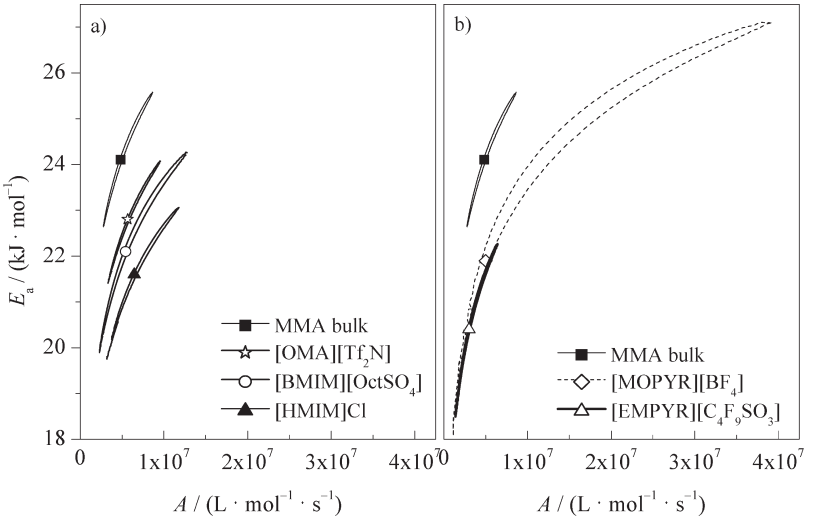

Figure 5. 95% joint confidence intervals and A and E_a indicated by the marker. The bulk data were taken from ref 37.

Table 3. Pre-exponential Factors, A, and Activation Energies, E_a, for MMA k_p, Number of k_p Values, N, Temperature Range, T, and k_p Values for MMA Polymerizations at 25 °C and $c_M = 2$ mol L^{-1}

solvent	N	T (°C)	E_a (kJ mol^{-1})	$A \times 10^{-6}$ (L mol^{-1} s^{-1})	k_p(25 °C) (L mol^{-1} s^{-1})
bulk[a]	16	10.3−64.0	24.1	4.8	288
[OMA][Tf$_2$N]	13	13.1−56.4	22.8	5.7	577
[MOPYR][BF$_4$]	6	10.9−55.5	21.9	5.0	728
[BMIM][OctSO$_4$]	8	11.9−55.6	22.1	5.4	725
[EMPYR][C$_4$F$_9$SO$_3$]	12	11.1−55.8	20.4	3.0	800
[HMIM]Cl	11	9.7−55.2	21.6	6.5	1068

[a] Bulk data from ref 37.

found for MMA/[EMPYR][C$_4$F$_9$SO$_3$] as shown in Figure 5b. Although the JCI for MMA/[MOPYR][BF$_4$] is very large (smallest number of data points), the system follows the same trend as the other data.

Furthermore, E_a values are lowered by up to 3.7 kJ mol^{-1} when replacing the monomer by ILs, while the pre-exponential factors with exception of [EMPYR][C$_4$F$_9$SO$_3$] are at most 35% higher than for the bulk system. Although a small difference between pre-exponential factors exists, the JCIs in Figure 5 suggest that it is the activation energy rather than the pre-exponential factor that causes the k_p enhancement for MMA polymerizations in ILs. The observed decrease in E_a for all polymerizations in ILs is in good agreement with literature data, where k_p values and Arrhenius parameters for MMA polymerizations in [BMIM][PF$_6$] and [BMIM][BF$_4$] were reported.[21,22] The decrease in E_a with the introduction of ILs as solvents in comparison to the bulk was also observed for glycidyl methacrylate polymerizations in [BMIM][BF$_4$] and [EMIM][EtSO$_4$].[22]

Discussion

Several theories were developed to explain the influence of organic solvents on propagation kinetics.[1,6,7,9,18,47−49] For nonaqueous systems, the most discussed are the "bootstrap" effect,[49] radical−solvent or monomer−solvent complexation,[1,18,48] and polarity effects.[21,22] The bootstrap effect is characterized by a significant difference in local and bulk monomer concentration due to differences in solvation of the polymer molecules by monomer and solvent. The occurrence of a local monomer concentration in the vicinity of the polymer radicals would result in an apparent variation in k_p as the bulk monomer concentration used to calculate k_p would deviate from the true value. For example, if the polymer is better solubilized by the monomer, the local monomer concentration would be higher than the overall monomer concentration in the system. If this difference is not accounted for, k_p values calculated are below the true k_p value. However, it was shown that even in the presence of the poor solvent supercritical carbon dioxide the maximum decrease in k_p is 40%.[7] Since MMA k_p for polymerizations in ILs increases by at least 100% compared to the bulk value (Table 2), the bootstrap effect does not seem to be a likely explanation for the k_p enhancement. Radical−solvent complexation may also be ruled out because complexed radical species are only expected to be formed if the complex is more stable than the radical itself. A stabilization of the radicals would lead to an increase in E_a and a lowering in k_p. However, the opposite effect is observed.

That leaves monomer−solvent complexation and polarity effects as possible explanations for the enhancement of MMA k_p due to the presence of ILs. To distinguish between these two theories, understanding of specific and nonspecific solvent−solute interactions is required. Moreover, the observed decrease in E_a in the presence of ILs suggests electronic effects to be responsible for the IL influence on MMA k_p. The rate coefficients may be affected by specific (such as hydrogen bonding and electron pair acceptor (EPA)−electron pair donator (EPD) interactions) and nonspecific (ion−dipole, dipole−dipole, dipole−induced dipole, and instantaneous dipole−induced dipole forces) solvent−solute interactions. To identify potential interaction sites between IL and monomer units, Figure 6 depicts an imidazolium, a pyridinium, and a trialkylammonium cation as well as a sulfate anion. In addition, Figure 6 illustrates which kind of interactions the ions may undergo. Scheme 2 gives canonical structures of the monomer and indicates possible interactions with the medium. The IL cations are able to interact not only with the associated anions via EPA−EPD, weak H−bond, and ion−ion interactions but also with the monomer through EPA/EPD, weak H-bond, and ion−dipole interactions. The nucleophilic anion may also interact with partially positively charged carbon atoms in MMA. Moreover, the C−H acidity of imidazolium

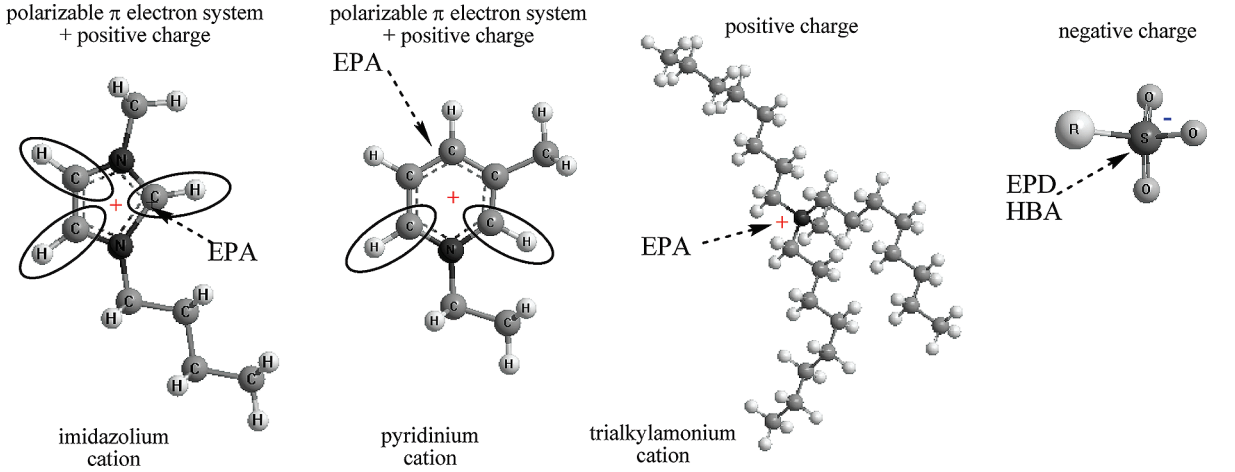

Figure 6. Structures and possible solvent−solute interactions of imidazolium, pyridinium, ammonium, and sulfate ions. The circles indicate the most acidic C−H bonds. EPA: electron pair acceptor; EPD: electron pair donator; HBA: H bond acceptor.

Scheme 2. Canonical Structures of MMA and Potential Sites for HBA (Hydrogen Bond Acceptor), HBD (Hydrogen Bond Donor), EPD (Electron Pair Donor), and EPA (Electron Pair Acceptor) Interactions

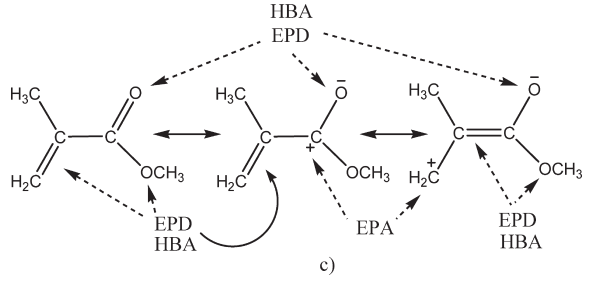

cations was discussed.[50−52] The H atoms circled in Figure 6 are somewhat capable of undergoing weak H bonding.

The importance of H bonding for the kinetics of radical polymerizations was discussed in previous publications.[1,5,6,18,53−58] In all aqueous systems a particular strong variation of k_p with monomer concentration by up to 1 order of magnitude is found.[53−58] The results were explained to be due to a competition between association of the carbonyl group of the growing chain with either monomer or water molecules. Association of the carbonyl groups with water results in less hindered rotational modes of the transition state structure due to the lower mass of water. As a consequence, the pre-exponential A is significantly enhanced in aqueous systems compared to the bulk systems. For a detailed discussion the reader is referred to the publications of Buback and co-workers, e.g., refs 53 and 57.

In nonaqueous systems the occurrence of H bonds involving OH groups resulted in an enhancement of k_p by at most 80%. It is well-known that ILs consisting of 1,3-dialkylimidazolium and to a lesser extent pyridinium cations may act as weak H-bond donors because of the weak acidic C(2)−H hydrogen atom at the heterocyclic ring.[35,59] It might be anticipated that H bonds are responsible for the variation of k_p for MMA polymerizations in IL. To probe for such H bonds involving carbonyl O atoms, vibrational spectroscopy is well-suited.[60] If H bonds are operative, a bimodal absorption peak occurs in the carbonyl region of the IR or Raman spectra. The peak indicative of nonassociated MMA carbonyl groups occurs at 1726 cm^{-1}, whereas associated carbonyl groups give rise to an absorption peak at lower wavenumbers around 1700 cm^{-1}.[22,60]

FTIR spectra recorded for the MMA/IL systems studied in this publication were measured at $c_M = 2$ mol L^{-1} and are shown in Figure 7. The IR spectra exhibit a monomodal peak assigned to

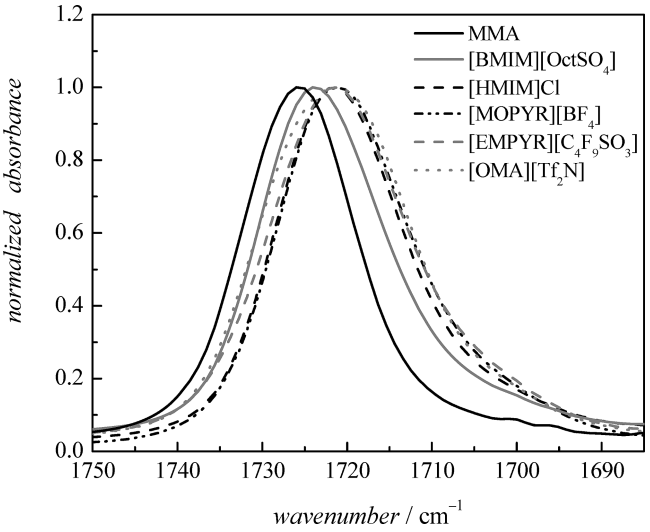

Figure 7. IR absorption band of the C=O stretching vibration of neat MMA and MMA/IL mixtures at $c_M = 2$ mol L^{-1} recorded at room temperature.

the carbonyl group in the absence of H bonds. Contributions from associated species giving rise to a peak at 1700 cm^{-1} are not seen. The finding is in agreement with previously reported data and confirms that H bonding is not responsible for the IL-induced enhancement of k_p.[22]

Besides being able to abandon the idea that H bonding is responsible for the IL influence on k_p, it needs to be tested whether information on other interactions between monomer and IL may be derived from the position of the absorption bands in the vibrational spectra. Previously, spectral data for a rather small number of systems only revealed that [EMIM][$EtSO_4$], [BMIM][BF_4], and [BMIM][PF_6] have the same influence on the carbonyl vibration of MMA and that the IL-induced shift of the carbonyl peak is stronger than for [EMIM][$HexSO_4$].[22] With a larger number of spectral and kinetic data at hand, it seems rewarding to check for a correlation between changes in spectral data and in the kinetic rate coefficients.

Table 2 shows that the peak maximum of the carbonyl vibration, ν_{max}(C=O), is shifted toward lower wavenumbers in the presence of ILs. A maximum shift of up to 6 cm^{-1} was detected. If ν_{max}(C=O) of MMA in [BMIM][$OctSO_4$] is compared to ν_{max}(C=O) of MMA in [BMIM][BF_4] and [BMIM]-[PF_6], it is clear that the shift of the carbonyl peak strongly

depends on the anion. ν_{max}(C=O) of MMA in [BMIM][$OctSO_4$] is shifted by only 2 cm^{-1} compared to the bulk MMA spectrum, whereas ν_{max}(C=O) of MMA is 4 cm^{-1} higher than in mixtures with 1-butyl-3-methylimidazolium-based ILs with the smaller anions BF_4^- and PF_6^-. The same is observed for the series of 1-ethyl-3-methylimidazolium-based ILs, [EMIM][$EtSO_4$], [EMIM][$HexSO_4$], and [EMIM][$OctSO_4$], where ν_{max}(C=O) gradually increases (1720, 1722, and 1723 cm^{-1}, respectively) with increasing anion chain length. This suggests that interactions of MMA and ILs become somewhat hindered as the anion size increases. For comparison, molar volumes of anions and cations taken from ref 44 or calculated according to ref 45 are contained in Table 2.

Similarly, the spectral data for ILs containing identical anions are compared. Generally, for the systems considered here the variations in ν_{max}(C=O) are less pronounced than the above-discussed anion-induced variations. The carbonyl peak maximum for MMA dissolved in [BMIM][BF_4] occurs at 1 and 2 cm^{-1} lower wavenumber than for MMA/[MOPYR][BF_4] and MMA/[MOIM][BF_4] mixtures, respectively. This finding implies that the smaller the cation, the stronger the variation of the carbonyl peak position.

The shift of the MMA carbonyl stretching vibration may be explained by alteration of the electron density of the C=O bond. The charge-separated canonical structures depicted in Scheme 2 are associated with slightly different energies of the carbonyl vibration and should be favored in the presence of ILs. In addition, electron density of the C=C will also be changed by the presence of ILs as C=O and C=C bonds form a conjugated system. However, in agreement with previous findings,[22] only small shifts of ν_{max}(C=C) by one or two wavenumbers were observed (see Table 2). Moreover, for MMA/[OMA][Tf_2N] mixtures no variation in ν_{max}(C=C) is found. At first sight this finding may be surprising. However, it needs to be considered that the extinction coefficient of the C=C bond is much lower than that of the carbonyl peak, which was indicated by the MMA spectrum given by Woecht et al.[22] Therefore, it is more difficult to identify changes of the weak peak assigned to C=C vibration. Because of the conjugated C=O and C=C double bond, however, the electron density of the C=C bond should also be affected by the presence of ILs. The alteration in electron density of the double bond results in changes of the monomer reactivity toward radical attack. It was stated that ester-substituted radicals are on the borderline between nucleophilic and electrophilic behavior and that the reaction with an alkene is enhanced due to either strong electron−acceptor or electron−donor substituents.[61,62] As a consequence, both cation and anion of the IL may contribute to an increase in k_p as both are able of favoring charge separated MMA resonance structures (see Scheme 2).

Figure 7 shows that not only the peak position is affected by the IL; to a larger extent the peak width of the carbonyl absorption is varied, too. To quantify this change, higher wavenumber half-band integrals of the C=O bonds were calculated and listed in Table 2. The most pronounced peak broadening occurs for MMA/[OMA][Tf_2N] mixtures. To explain the significant broadening, it should be considered that in case of [OMA][Tf_2N] both cation and anion are very bulky and the charges are sterically shielded. In addition, the cation is also highly unsymmetrical as it has three long octyl chains and one methyl group attached to the nitrogen. Interactions between ammonium cations and monomer molecules in the vicinity of the N−CH_3 bond will contribute to changes in electron density of MMA carbonyl bonds, which result in a shift of ν_{max}(C=O). In addition, monomer molecules may be situated in the vicinity of longer octyl chains of the cations and, thus, are not able to strongly interact with the positive cation core. As a consequence, ν_{max}(C=O) of these monomer molecules is the same as in the bulk system. The resulting broad peak associated with the carbonyl vibration reflects a superposition of carbonyl peaks originating from different interactions between monomer and cation. The absorption peak related to the C=C double bond is generally broader, and no clear trend in variation with the various systems is found.

Scheme 3. Molecular Structure and Potential Interaction Sites of Reichardt's Dye Taken from Ref 35

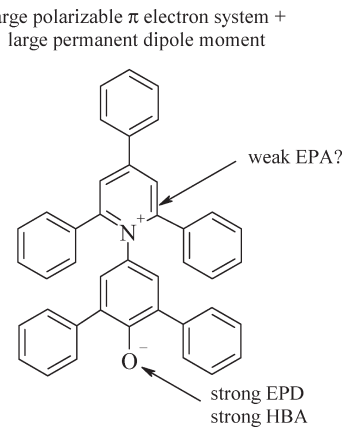

Comparison of ν_{max}(C=O) for a series of ILs containing the same cation with the propagation rate coefficients derived from PLP experiments in these ILs indicates that the lower the ν_{max}(C=O), the higher the IL-induced enhancement of k_p. However, in case of polymerizations in [BMIM][BF_4] and [BMIM][PF_6] ν_{max}(C=O) values are identical, while some differences in k_p occur. Moreover, the data listed in Table 2 show that a universal correlation between ν_{max}(C=O) and k_p is not existing. The carbonyl peak of MMA in solution with [HMIM]Cl or [OMA][Tf_2N] is seen at 1721 cm^{-1}, but k_p is enhanced by a factor of 3.8 or 2.0, respectively. This example indicates that the IR data are not sufficient to reliably estimate the solvent induced variation in MMA k_p.

The data in Table 2 suggest that the variation in k_p scales with the size of the ions: the larger the ions, the smaller the IL-induced enhancement of k_p. The largest increase in k_p by a factor of 4 is seen for polymerizations in [EMIM][$EtSO_4$], [BMIM][BF_4]], and [HMIM]Cl. The findings suggest that polarity plays an important role; however, a more sophisticated analysis is required. It should be noted that the increase in MMA k_p with decreasing IL size in this study and the enhancement of MMA k_p with increasing size of organic solvent molecules reported in ref 10 are not in conflict. In our previous work solvents were chosen that do not undergo specific interactions with the monomer or macroradical. The solvent induced-changes in k_p were assigned to local monomer concentrations being different from the overall monomer concentration. In the present work interactions between anions and cations with monomer units are expected to occur (see below). The different origin of the IL- and solvent-induced changes in k_p is also reflected in the degree of enhancement: organic solvents led to a maximum increase in k_p by 80%, whereas ILs may increase k_p by a factor of 4 at comparable monomer concentrations.

As pointed out by Reichardt, often a single physical parameter is not sufficient to characterize a substance with respect to its solvent properties.[35,36] To account for contributions from Coulomb forces and from specific interactions such as hydrogen bonding and electron pair donor (EPD)−electron pair acceptor (EPA) interactions, the overall solvation capability of a solvent should be considered. To probe for these interactions, UV−vis spectra of solvatochromic dyes dissolved in the solvent of interest may be recorded. Reichardt's dye given in Scheme 3 is suitable for registration of dipole/dipole and dipole/induced dipole

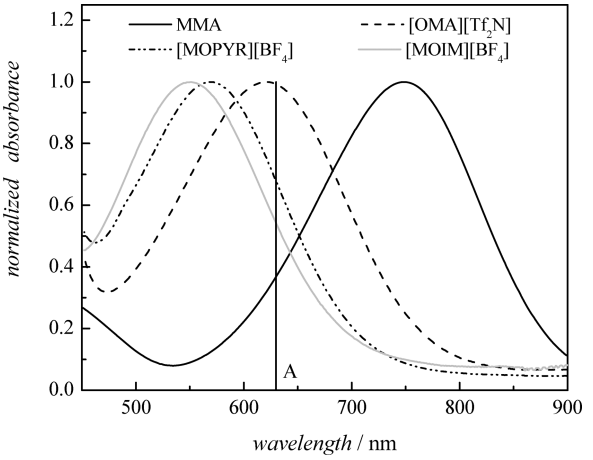

Figure 8. Longest wavelength intramolecular charge-transfer $\pi-\pi^*$ absorption band of Reichardt's dye in MMA, [MOPYR][BF_4], [OMA][Tf_2N], and [MOIM][BF_4]. A: λ_{max} for dimethyl sulfoxide.[65]

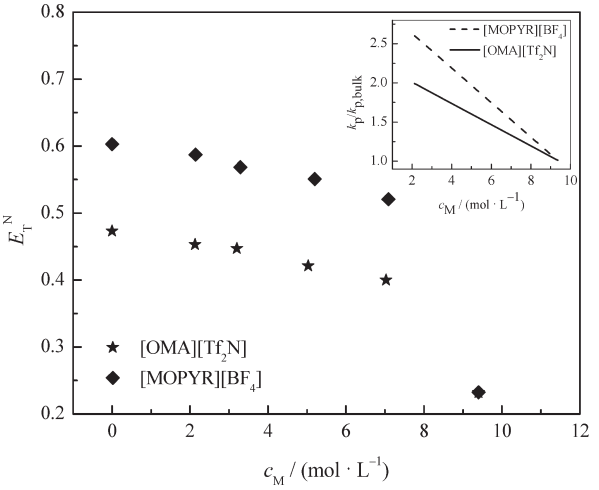

Figure 9. E_T^N values for mixtures of MMA with [OMA][Tf_2N] or [MOPYR][BF_4] derived from UV−vis spectra. The inset gives the variation of the corresponding $k_p/k_{p,bulk}$ values.

interactions as it exhibits a large permanent dipole. Moreover, it has a large polarizable π-system being suitable for detection of dispersion interactions, and the phenolate oxygen atom may interact with H-bond donors and electron pair acceptors.

As an example, UV−vis absorption spectra of Reichardt's dye dissolved in MMA, [MOPYR][BF_4], [OMA][Tf_2N], and [MOIM][BF_4] are presented in Figure 8. The UV−vis spectra measured in the ILs are significantly shifted to lower wavelength compared to MMA. The weakest shift of around 127 nm is found for [OMA][Tf_2N], whereas [MOPYR][BF_4] and [MOIM][BF_4] cause a stronger shift of 179 and 194 nm, respectively. The position of the peak maxima in UV−vis spectra of all systems investigated, λ_{max}, and E_T^N are contained in Table 2. The lowest values of λ_{max} ranging from 545 to 549 nm were determined for [EMIM][$EtSO_4$], [EMIM][HexSO4], [BMIM][BF_4], and [BMIM][PF_6]. Table 2 shows that E_T^N values for all imidazolium-based ILs except for [HMIM]Cl are in the range from 0.63 to 0.68. [HMIM]Cl constitutes an exception because of the small anion associated with a very high charge density. As a consequence, the cation−anion interactions are stronger than in all other ILs used in this work.[63] Because of the stronger cation−anion interactions, [HMIM]Cl shows the highest viscosity of 8000 mPa·s at 25 °C, which is about 7.5 times higher than the viscosity of [BMIM][$OctSO_4$], the second most viscous IL used in this study.[64] The stronger anion−cation interactions in case of [HMIM]Cl influence its interactions with the dye and is finally reflected in the significantly different E_T^N value.

[MOPYR][BF_4] has a slightly lower E_T^N than the 1-butyl-3-methylimidazolium- and 1-ethyl-3-methylimidazolium-based ILs. The lowest E_T^N value among the ILs listed in Table 2 has [OMA][Tf_2N]. As already mentioned above, both cation and anion of [OMA][Tf_2N] are very bulky, which may significantly hinder its interaction with other molecules. In addition, [OMA][Tf_2N] does not have a polarizable ring and has a lower H-bond donating ability than imidazolim- or pyridinium-based ILs used in this study. As a result, interactions between [OMA][Tf_2N] and MMA are of a lower intensity than in all other systems, which is associated with the lowest enhancement in k_p among the investigated ILs.

Even though E_T^N values of all ILs were suggested to be dominated by the cation,[28] an influence of the anion is clearly observed. The data listed in Table 2 show that E_T^N decreases as the anion size increases in the analogue series of for 1-butyl-3-methylimidazolium- and 1-ethyl-3-methylimidazolium-based ILs. This finding suggests that IL interactions with the dye are being reduced with larger sizes of the anion. The same may apply to IL interactions with MMA, which may explain the finding that $k_p/k_{p,bulk}$ is the higher the smaller the anion.

If ILs composed of the same anion, e.g., tetrafluoroborate, are compared, the highest E_T^N refers to [BMIM][BF_4]. [MOIM][BF_4] with the longest alkyl chain at the imidazolium ring has a slightly lower E_T^N than the IL with 1-butyl-3-methylimidazolium cation. The lowest E_T^N corresponds to the pyridinium-based IL, [MOPYR][BF_4]. Again, $k_p/k_{p,bulk}$ values follow the E_T^N changes—the lower the E_T^N, the lower the associated $k_p/k_{p,bulk}$ value. The difference in E_T^N between [EMIM][$OctSO_4$] and [BMIM][$OctSO_4$] is negligible as the cations are very similar and the anion is rather large.

Although $k_p/k_{p,bulk}$ used for comparison were derived from PLP at rather dilute solution, it seemed important to determine E_T^N values of some MMA/IL mixtures. The variation of E_T^N with monomer concentration for MMA mixtures with [OMA][Tf_2N] and [MOPYR][BF_4] is depicted in Figure 9. For comparison, the inset gives the variation of $k_p/k_{p,bulk}$ with c_M. It is clearly seen that E_T^N increases significantly with the addition of IL. While a linear variation of E_T^N with c_M is found for concentrations between pure IL and around 7 mol L^{-1} MMA, E_T^N for bulk MMA is significantly lower than all other E_T^N values. This finding is in agreement with studies on, e.g., mixtures of ILs with 2-butanone.[66] For both MMA/IL systems studied here, linear fitting of the data for the mixtures results in parallel lines. Contrary experimental k_p data may be well represented by a linear fit including the pure MMA value (see the inset of Figure 9).

Although there is a mismatch for the variation of E_T^N with c_M and $k_p/k_{p,bulk}$ with c_M at high monomer concentrations, it seemed rewarding to test how k_p varies with E_T^N. Figure 10 gives the variation of k_p for polymerizations at $c_M = 2$ mol L^{-1} with E_T^N derived from the pure ILs (open symbols) and for polymerizations in [OMA][Tf_2N] and in [MOPYR][BF_4] at different c_M with E_T^N derived for the monomer/IL mixtures at c_M of the polymerization (filled symbols). The dotted line included in Figure 10 to guide the eye shows that only a general trend of an increase in k_p with increasing E_T^N is found. Figure 10 indicates that a master correlation for the prediction of k_p for polymerizations in ILs cannot be given. Although E_T^N values account for different types of interactions, the polarity influence on k_p is still too complex to be represented by a single parameter equation based only on E_T^N. As already discussed, MMA k_p for polymerizations in ILs is influenced by both the anion and the cation. However, E_T^N parameters may not be representative of the anion properties.[28,67]

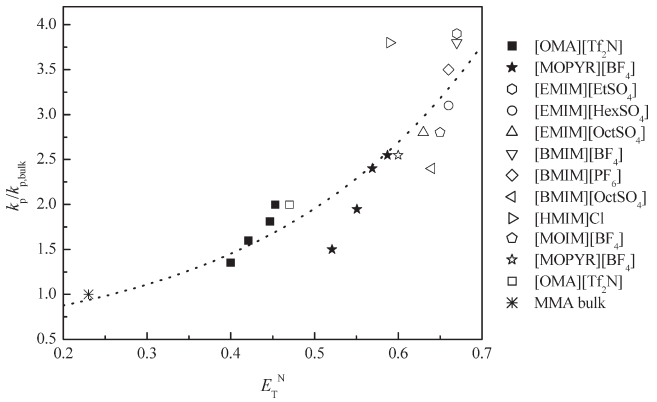

Figure 10. Variation of $k_p/k_{p,bulk}$ with E_T^N. Open symbols refer to a monomer concentration of 2 mol L^{-1} and E_T^N determined for pure ILs or MMA, filled systems to concentrations ≥ 2 mol L^{-1}, and E_T^N derived for the MMA/IL mixtures.

Furthermore, E_T^N reflects both specific (EPA-EPD, H bonding) and nonspecific interactions. Each of them may contribute to the observed enhancement of MMA k_p to a different extent. For a quantitative understanding of the solvent dependent data, a more rigorous approach to the treatment of polarity effects has to be applied. For example, a linear solvation energy relationship proposed by Kamlet, Abboud, and Taft breaks down polarity into dipolarity and polarizability, HBD acidity, and HBA basicity.[68] Using such a multiparameter equation for the correlation of solvent properties and solvent induced variations in k_p may provide a tool for the description and in future prediction of the propagation rate coefficients. Currently, these investigations are underway.

It seemed rewarding to discuss the data from this study together with previously published k_p values for solution polymerizations that differed strongly from the corresponding bulk values. As IR of MMA/IL systems did not give any indication for the presence of H bonds, the origin of MMA k_p enhancement in ILs seems to have some similarities with k_p enhancement in DMSO. For comparison with MMA/IL systems, the position of λ_{max} for DMSO[67] was included in Figure 8 (marked by A in the graph). Figure 8 shows that λ_{max} of DMSO is slightly higher than λ_{max} of [OMA][Tf_2N]. Interactions between Reichardt's dye and DMSO are dominated by EPA−EPD interactions as well as on nonspecific interactions. It is worth mentioning that both DMSO and [OMA][Tf_2N] lead to a 2-fold increase in k_p. Another example for EPA−EPD interactions being responsible for a solvent induced increase in k_p is MMA polymerizations in other sulfur containing solvents such as 2,6-dithiaheptane and 1,5-dithiacyclooctane.[9] The enhancement of k_p amounts up to a factor of 2, comparable to that in the presence of DMSO or [OMA][Tf_2N].

Conclusions

The studies into the IL influence on the propagation kinetics in MMA polymerizations indicate a significant enhancement of k_p and a lowering of the associated activation energies compared to the bulk systems in all cases. k_p values for polymerizations with $c_M = 2$ mol L^{-1} increase by a factor of 2−4 depending on the type of IL used. Generally, the enhancement of k_p is the larger the smaller the ions of the IL. The increase in k_p may qualitatively be predicted by the polarity of the ILs, by considering vibrations of the carbonyl group of the monomer, or from UV−vis spectra of Reichardt's dye dissolved in ILs. However, the single E_T^N parameter is not sufficient to quantitatively correlate k_p and the solvent properties of the ILs. Currently, it is tested whether a multiparameter representation of the solvent may allow for a better correlation between the kinetic data and the solvent properties.

Acknowledgment. A.J. and S.B. gratefully acknowledge financial support by University of Potsdam in the framework of the Graduate School on Green Chemistry and are very grateful to Prof. Dr. Hans-Gerd Löhmannsröben, University of Potsdam, for access to the laser and the UV spectrometer. Experimental assistance by Christian Brendler and Diana Hill is acknowledged. N.G. thanks the Spanish Ministry of Science and Technology for funding (Programma "Ramón y Cajal" and MAT2008-06725-C03-01).

Supporting Information Available: Full experimental data for all PLP experiments. This material is available free of charge via the Internet at http://pubs.acs.org.

References and Notes

(1) Kamachi, M. *Adv. Polym. Sci.* **1981**, *38*, 55.
(2) Kamachi, M.; Liaw, D. J.; Nozakura, S. *Polym. J.* **1981**, *13*, 41.
(3) Olaj, O. F.; Schnöll-Bitai, I. *Monatsh. Chem.* **1999**, *130*, 731.
(4) Zammit, M. D.; Davis, T. P.; Willett, G. D.; O'Driscoll, K. F. *J. Polym. Sci., Part A: Polym. Chem.* **1997**, *35*, 2311.
(5) Beuermann, S. *Macromolecules* **2004**, *37*, 1037.
(6) Beuermann, S.; Nelke, D. *Macromol. Chem. Phys.* **2003**, *204*, 460.
(7) Beuermann, S.; Buback, M.; El Rezzi, V.; Jürgens, M.; Nelke, D. *Macromol. Chem. Phys.* **2004**, *205*, 876.
(8) Morrison, D. A.; Davis, T. P. *Macromol. Chem. Phys.* **2000**, *201*, 2128.
(9) Harrisson, S.; Barner-Kowollik, C.; Davis, T. P.; Evans, R. A.; Rizzardo, E.; Stenzel, M.; Yin, M. *Z. Phys. Chem. (Munich)* **2005**, *219*, 267.
(10) Beuermann, S.; García, N. *Macromolecules* **2004**, *37*, 3018.
(11) Beuermann, S.; Buback, M.; Hesse, P.; Kuchta, F.-D.; Lacík, I.; van Herk, A. M. *Pure Appl. Chem.* **2007**, *79*, 1463.
(12) Lacík, I.; Beuermann, S.; Buback, M. *Macromol. Chem. Phys.* **2004**, *205*, 1080.
(13) Olaj, O. F.; Bitai, I.; Hinkelmann, F. *Makromol. Chem.* **1987**, *188*, 1689.
(14) Buback, M.; Gilbert, R. G.; Russell, G. T.; Hill, D. J.; O'Driscoll, K. F.; Shen, J.; Winnik, M. A. *J. Polym. Sci., Part A: Polym. Chem.* **1992**, *30*, 851.
(15) Beuermann, S.; Buback, M.; Davis, T. P.; Gilbert, R. G.; Hutchinson, R. A.; Olaj, O. F.; Russell, G. T.; Schweer, J.; van Herk, A. M. *Macromol. Chem. Phys.* **1997**, *198*, 1545.
(16) Buback, M.; Gilbert, R. G.; Hutchinson, R. A.; Klumperman, B.; Kuchta, F.-D.; Manders, B. G.; O'Driscoll, K. F.; Russell, G. T.; Schweer, J. *Macromol. Chem. Phys.* **1995**, *196*, 3267.
(17) Beuermann, S.; Buback, M.; Russell, G. T. *Macromol. Rapid Commun.* **1994**, *15*, 647.
(18) O'Driscoll, K. F.; Monteiro, M. J.; Klumperman, B. *J. Polym. Sci., Part A: Polym. Chem.* **1997**, *35*, 515.
(19) Harrisson, S.; Kapfenstein-Doak, H.; Davis, T. P. *Macromolecules* **2001**, *34*, 6214.
(20) Harrisson, S.; Mackenzie, S. R.; Haddleton, D. M. *Chem. Commun.* **2002**, 2850.
(21) Harrisson, S.; Mackenzie, S. R.; Haddleton, D. M. *Macromolecules* **2003**, *36*, 5072.
(22) Woecht, I.; Schmidt-Naake, G.; Beuermann, S.; Buback, M.; García, N. *J. Polym. Sci., Part A: Polym. Chem.* **2008**, *46*, 1460.
(23) Andrzejewska, E.; Podgorska-Golubska, M.; Stepniak, I.; Andrzejewski, M. *Polymer* **2009**, *50*, 2040.
(24) Hong, K.; Zhang, H.; Mays, J. W.; Visser, A. E.; Brazel, C. S.; Holbrey, J. D.; Reichert, W. M.; Rogers, R. D. *Chem. Commun.* **2002**, 1368.
(25) Strehmel, V.; Laschewsky, A.; Wetzel, H.; Görnitz, E. *Macromolecules* **2006**, *39*, 923.
(26) Lachwa, J.; Szydlowski, J.; Najdanovic-Visak, V.; Rebelo, L. P. N.; Seddon, K. R.; Nunes , M.; Esperança, J. M. S. S.; Guedes, H. J. R. *J. Am. Chem. Soc.* **2005**, *127*, 6542.
(27) Gutowski, K. E.; Broker, G. A.; Willauer, H. D.; Huddleston, J. G.; Swatloski, R. P.; Holbrey, J. D.; Rogers, R. D. *J. Am. Chem. Soc.* **2003**, *125*, 6632.
(28) Scurto, A. M.; Aki, S. N. V. K.; Brennecke, J. F. *J. Am. Chem. Soc.* **2002**, *124*, 10276.

(29) Wasserscheid, P.; Welton, T. *Ionic Liquids in Synthesis*; Wiley-VCH Verlag GmbH & Co.: Berlin, 2008.
(30) Baranyai, K. J.; Daecon, G. B.; MacFarlane, D. R.; Pringle, J. M.; Scott, J. L. *Aust. J. Chem.* **2004**, *57*, 145.
(31) Earle, M. J.; Seddon, K. R. *Pure Appl. Chem.* **2000**, *72*, 1391.
(32) Kubisa, A. *Prog. Polym. Sci.* **2004**, *29*, 3.
(33) Shen, Y.; Ding, S. *Prog. Polym. Sci.* **2004**, *29*, 1053.
(34) Lu, J.; Yan, F.; Texter, J. *Prog. Polym. Sci.* **2009**, *34*, 431.
(35) Reichardt, C. *Chem. Soc. Rev.* **1992**, 147.
(36) Reichardt, C. *Green Chem.* **2005**, *7*, 339.
(37) García, N.; Tiemblo, P.; Guzmán, J. *Macromolecules* **2007**, *40*, 4802.
(38) Hutchinson, R. A.; Beuermann, S.; Paquet, D. A. Jr.; McMinn, J. H. *Macromolecules* **1997**, *30*, 3490.
(39) Hutchinson, R. A.; McMinn, J. H.; Paquet, D. A. Jr.; Beuermann, S.; Jackson, C. *Ind. Eng. Chem. Res.* **1997**, *36*, 1103.
(40) Harrod, W. B.; Pienta, N. J. *J. Phys. Org. Chem.* **1990**, *3*, 534.
(41) Beuermann, S.; Buback, M.; Russell, G. T. *Macromol. Chem. Phys.* **1995**, *196*, 2493.
(42) Susan, A. B. H.; Kaneko, T.; Noda, A.; Watanabe, M. *J. Am. Chem. Soc.* **2005**, *127*, 4976.
(43) Crowhurst, L.; Mawdsley, P. R.; Pérez-Arlandis, J. M.; Salter, P. A.; Welton, T. *Phys. Chem. Chem. Phys.* **2003**, *5*, 2790.
(44) Kobrak, M. N. *Green Chem.* **2008**, *10*, 80.
(45) Ye, C.; Shreeve, J. M. *J. Phys. Chem. A* **2007**, *111*, 1456.
(46) van Herk, A. M. *J. Chem. Educ.* **1995**, *72*, 138.
(47) Bamford, C. H.; Brumby, S. *Makromol. Chem.* **1967**, *105*, 122.
(48) Henrici-Olivé, G.; Olivé, S. *Makromol. Chem.* **1963**, *68*, 219.
(49) Harwood, H. J. *Macromol. Symp.* **1987**, *10/11*, 331.
(50) Schmidt-Naake, G.; Woecht, I.; Schmalfuβ, A.; Glück, T. *Macromol. Symp.* **2009**, 204.
(51) Holomb, R.; Martinelli, A.; Albinsson, I.; Lassègues, J. C.; Johansson, P.; Jacobsson, P. *J. Raman Spectrosc.* **2008**, *39*, 793.
(52) Dong, K.; Zhang, S.; Wang, D.; Yao, X. *J. Phys. Chem. A* **2006**, *110*, 9775.
(53) Beuermann, S.; Buback, M.; Hesse, P.; Lacík, I. *Macromolecules* **2006**, *39*, 184.
(54) Beuermann, S.; Buback, M.; Hesse, P.; Kukučková, S.; Lacík, I. *Macromol. Symp.* **2007**, *248*, 41.
(55) Beuermann, S.; Buback, M.; Hesse, P.; Kuchta, F.-D.; Lacik, I.; van Herk, A. M. *Pure Appl. Chem.* **2007**, *79*, 1463.
(56) Buback, M.; Hesse, P.; Hutchinson, R. A.; Kasak, P.; Lacik, I.; Stach, M.; Utz, I. *Ind. Eng. Chem. Res.* **2008**, *47*, 8197.
(57) Stach, M.; Lacík, I.; Chorvat, D.Jr.; Buback, M.; Hesse, P.; Hutchinson, R. A.; Tang, L. *Macromolecules* **2008**, *41*, 5174.
(58) Seabrook, S. A.; Tonge, M. P.; Gilbert, R. G. *J. Polym. Sci., Part A: Polym. Chem.* **2005**, *43*, 1357.
(59) Lee, J.-M.; Ruckes, S.; Prausnitz, J. M. *J. Phys. Chem. B* **2008**, *112*, 1473.
(60) Buback, M.; Mähling, F. O. *J. Supercrit. Fluids* **1995**, *8*, 119.
(61) Giese, B.; He, J.; Mehl, W. *Chem. Ber.* **1988**, *121*, 2063.
(62) Baciocchi, E.; Floris, B.; Muraglia, E. *J. Org. Chem.* **1993**, *58*, 2013.
(63) Avent, A. G.; Chaloner, P. A.; Day, M. P.; Seddon, K. R.; Welton, T. *J. Chem. Soc., Dalton Trans.* **1994**, 3405.
(64) Material safety data sheet, Solvent Innovation, 2008.
(65) Fletcher, K. A.; Storey, I. A.; Hendricks, A. E.; Pandey, S.; Pandey, S. *Green Chem.* **2001**, *3*, 210.
(66) Mellein, B. R.; Aki, S. N. V. K.; Ladewski, R. L.; Brennecke, J. F. *J. Phys. Chem. B* **2007**, *111*, 131.
(67) Muldoon, M. J.; Gordon, C. M.; Dunkin, I. R. *J. Chem. Soc., Perkin Trans.* **2001**, *2*, 433.
(68) Kamlet, M. J.; Abboud, J.-L. M.; Abraham, M. H.; Taft, R. W. *J. Org. Chem.* **1983**, *48*, 2887.